

Radwan Khawaled · Andrew Bruening-Wright
John P. Adelman · James Maylie

Bicuculline block of small-conductance calcium-activated potassium channels

Received: 12 January 1999 / Received after revision: 29 March 1999 / Accepted: 31 March 1999

Abstract Small-conductance calcium-activated potassium channels (SK channels) are gated solely by intracellular calcium ions and their activity is responsible for the slow afterhyperpolarization (AHP) that follows an action potential in many excitable cells. Brain slice studies commonly employ a methyl derivative of bicuculline (bicuculline-m), a GABA_A (γ -aminobutyric acid) receptor antagonist, to diminish the tonic inhibitory influences of GABAergic synapses, or to investigate the role of these synapses in specialized neural networks. However, recent evidence suggests that bicuculline-m may not be specific for GABA_A receptors and may also block the slow AHP. Therefore, the effects of bicuculline-m on cloned apamin-sensitive SK2 and apamin-insensitive SK1 channels were examined following expression in *Xenopus* oocytes. The results show that at concentrations employed for slice recordings, bicuculline-m potently blocks both apamin-sensitive SK2 currents and apamin-insensitive SK1 currents when applied to outside-out patches. Apamin-insensitive SK1 currents run down in excised patches. The potency of bicuculline-m block also decreases with time after patch excision. Site-directed mutagenesis that changes two residues in the outer vestibule of the SK1 pore that confers apamin sensitivity also reduces run down of the current in patches, and endows stable sensitivity to bicuculline-m indistinguishable from SK2. Therefore, the use of bicuculline-m in slice recordings may mask apamin-sensitive slow AHPs that are important determinants of neuronal excitability. In addition, bicuculline-m-insensitive slow AHPs may indicate that the underlying channels have run down.

Key words Bicuculline block · GABA_A receptors · Slow afterhyperpolarization · SK channels

Introduction

In many neurons, the action potential is followed by a slow afterhyperpolarization (slow AHP), which is due to the activation of small-conductance calcium-activated potassium channels (SK channels). SK channels are not gated by voltage and are activated by submicromolar concentrations of intracellular calcium. In the sustained presence of excitatory neurotransmitter, the slow AHP becomes increasingly prominent, reflecting the continued increase of intracellular calcium levels, until the cell is no longer able to reach threshold for a subsequent action potential, a phenomenon termed spike-frequency adaptation, an important regulator of excitability [4, 11, 24, 27]. Two types of slow AHPs may be distinguished. In many neurons, such as hippocampal interneurons [40], the slow AHP is sensitive to the bee venom toxin apamin, has relatively faster kinetics and is not regulated by neurotransmitters. In hippocampal pyramidal neurons, the slow AHP is insensitive to apamin, exhibits very slow kinetics, and is modulated by neurotransmitter-induced second messengers such as protein kinase A (PKA) [17, 20, 23]. These two types of slow AHPs are not mutually exclusive, as apamin-sensitive and apamin-insensitive transmitter-regulated components are present in many neurons such as vagal motoneurons [29], neocortical neurons [19], and pyramidal neurons of the sensorimotor cortex [30].

Brain slice preparations are commonly used for studies of synaptic transmission. An attractive feature of the slice preparation is that much of the intrinsic neuronal circuitry remains functionally intact, including inhibitory, GABAergic synapses. In brain slice and other tissue preparations, many investigators have included bicuculline, an antagonist of GABA_A receptor channels, in the solution bathing the slice to improve stimulus-evoked responses, or to probe the role of GABA_A receptor chan-

R. Khawaled · A. Bruening-Wright · J.P. Adelman
Vollum Institute, Oregon Health Sciences University,
3181 S.W. Sam Jackson Park Road, Portland, OR 97201, USA

J. Maylie (✉)
Department of Obstetrics and Gynecology,
Oregon Health Sciences University; L-458,
3181 S.W. Sam Jackson Park Road, Portland, OR 97201, USA
e-mail: mayliej@ohsu.edu
Tel.: +1-503-4942106, Fax: +1-503-4945296

nels in synaptic responses [5, 15, 22, 25, 32, 34, 35, 36,37]. Bicuculline is supplied as either the free base or a methyl derivative (herein referred to bicuculline-m) which uses either chloride, bromide, or iodide as the counter-ion; the salts are water soluble and are the most widely employed.

It has been assumed that bicuculline is a specific GABA_A antagonist; however, several reports have suggested that in addition to the antagonism of GABA_A receptor channels, bicuculline-m also blocks the slow AHP. Recordings from dopamine neurons in the ventral tegmental area and the substantia nigra pars compacta have shown that bicuculline-m, but not picrotoxin (another GABA_A antagonist), blocks the apamin-sensitive slow AHP. This effect persists in the presence of tetrodotoxin (TTX), suggesting that it is not due to reduced calcium entry but rather a direct effect on the SK channels [31]. Bicuculline-m also potentiates the NMDA-dependent burst firing in these neurons by reducing the slow AHP, similar to the effects of apamin [14]. In thalamic reticular neurons, where the role of GABAergic inhibitory synapses in thalamocortical synchronization has been examined using bicuculline-m [15,36], the methiodide, methbromide, and methylchloride salts enhance the low-threshold calcium spike, not seen with picrotoxin, and which persists in the presence of TTX; this effect is caused by block of the current underlying the slow AHP, I_{sAHP} [9].

These results suggest that bicuculline-m may directly block the channels underlying the slow AHP. Three SK channels have been cloned and reflect the different pharmacologies of the slow AHP in neurons: SK2 and SK3 channels are apamin-sensitive, while SK1 channels are apamin-insensitive [13,16]. Therefore, we examined the

effects of bicuculline methylchloride and the bicuculline free base on the cloned SK channels.

Materials and methods

Xenopus care and handling were in accordance with the highest standards of institutional guidelines. Frogs underwent no more than two surgeries, separated by at least 3 weeks, and surgeries were performed using well-established techniques. Frogs were anesthetized with an aerated solution of 3-aminobenzoic acid ethyl ester. Oocytes were studied 2–8 days after injection with 0.2 ng mRNA. In vitro mRNA synthesis and oocyte injections were performed as previously described [1]. Outside-out macropatch recordings were made at room temperature (approximately 23°C) with electrodes pulled from thin-walled, filamented borosilicate glass (World Precision Instruments) and filled with 120 mM K-gluconate, 5 mM HEPES, (pH 7.2, adjusted with KOH) supplemented with CaCl₂ to give a free Ca²⁺ concentration of 10 μM; the proportion of calcium binding to gluconate was determined assuming a stability constant for calcium gluconate of 15.9 M⁻¹ [8]. To obtain Ca²⁺ concentrations below 1 μM, 1 mM EGTA was added to the internal solution and CaCl₂ was added as calculated using published stability constants [21]. Electrode resistance was typically 1–3 MΩ. Excised patches were superfused with a solution containing 120 mM K-gluconate, 5 mM HEPES (pH 7.2, adjusted with KOH). Patch formation and excision were performed within ≤ 30 s and drugs were applied by positioning the patch in front of a series of flow pipes allowing for a solution exchange in approximately 1 s. Voltage-clamp recordings were performed with an Axopatch 1B-100/1 headstage (Axon Instruments) or an EPC9 patch-clamp amplifier (HEKA electronics). The data were low-pass Bessel filtered at 2 kHz and acquired using Pulse software (HEKA Elektronik). Currents elicited by 2-s voltage ramps between the potentials indicated in the text were acquired at a sampling frequency of 1 kHz. Data analysis was performed using Pulse (HEKA) and IGOR (Wavemetrics). Concentration/response curves were obtained as follows: current amplitudes were measured at the indicated voltage and corrected for run down as indicated in the text, data were normalized to the average of the con-

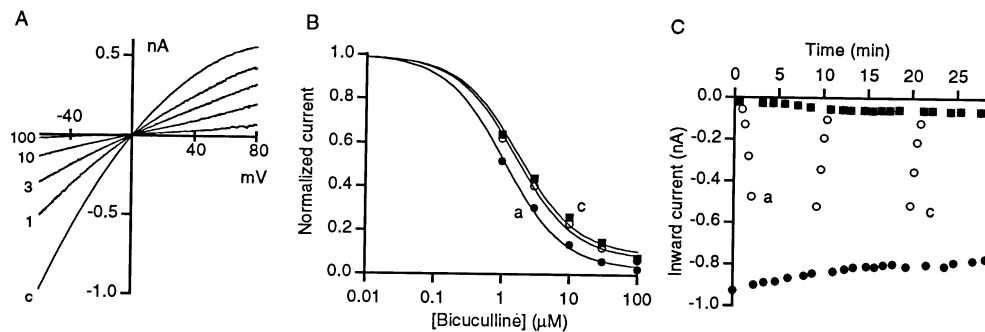


Fig. 1A–C Concentration/response relationship of bicuculline-m block of small-conductance calcium-activated potassium channels (SK2). **A** Current traces elicited by a 2-s voltage ramp from -60 to 80 mV from an outside out macropatch excised from an oocyte expressing SK2. The traces were obtained in control solution (*c*) and in the presence of 1, 3, 10, 100 μM bicuculline-m (labeled accordingly) within the first 2 min following patch excision. **B** Bicuculline-m concentration/response curves measured at three times following patch excision (response curves labeled *a* and *c* correspond to time points in panel **C**). The current measured at -60 mV was normalized by the response in the control solution prior to each series and plotted as a function bicuculline-m concentration.

Nonlinear least-squares fit to a Langmuir isotherm (*continuous line*) yielded an IC₅₀ of 1.1, 1.6 and 1.8 μM for *a*, *b* and *c*, respectively. An offset was included to account for residual, unblocked current which increased during the time course of recording (**C**) from 0.03 in *series a* to 0.09 in *series c*. *Series a* is measured from the current traces in panel **A**. **C** Time dependence of inward current recorded at -60 mV as a function of time following patch excision. Plotted are current values in control solution (*closed circles*), 100 μM bicuculline-m (*closed squares*) and three concentrations/response curves to 1, 3, 10, and 30 μM bicuculline-m (*open circles*). The first and last series are indicated by *a* and *c*

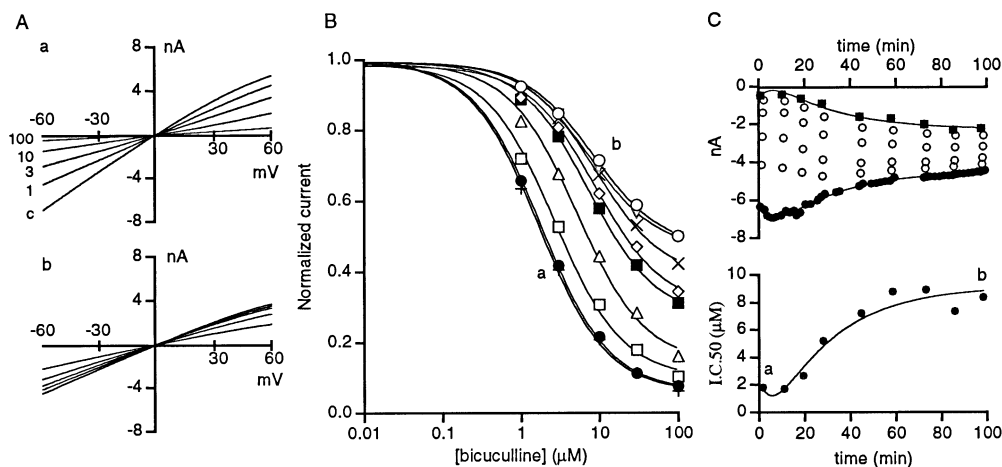


Fig. 2A–C Bicuculline-m-induced block of SK1 decreases with time following patch excision. **A** Current traces elicited by a 2-s voltage ramp from -60 to 60 mV from an outside out macropatch excised from an oocyte expressing SK1. The traces were obtained in control solution (*c*) and in the presence of 1, 3, 10, 100 μM bicuculline-m (labeled accordingly) within the first 2 min (**Aa**) and 100 min (**Ab**) following patch excision. **B** Bicuculline-m concentration/response curves at -60 mV measured at increasing times following patch excision (response curves labeled *a* and *b* correspond to first and last series illustrated in **A** and to the time points labeled *a* and *b* in **C**). The shift in the concentration/response curve corresponds to increasing time following patch excision. Nonlinear least-squares fit to a Langmuir isotherm (continuous line) yielded an increase in IC_{50} from 1.7 to 8.4 μM measured 2 min and 98 min following patch excision (*a* and *b*, respectively). The fraction of SK1 not blocked by bicuculline-m increased from 0.06 to 0.44 between *a* and *b*. **C** Time dependence of inward cur-

rent recorded at -60 mV (upper panel) and IC_{50} from concentration/response curves in **B** (lower panel) as a function of time following patch excision. Plotted in the upper panel are current values in control solution (closed circles), 100 μM bicuculline-m (closed squares) and nine concentration/response curves to 1, 3, 10, and 30 μM bicuculline-m (open circles). The first and last series are indicated by *a* and *b* in the upper and lower panels. The time course of run down of the control data was described by a sum of two exponentials (continuous line through closed circles, upper panel) which was used to correct for run down as described in the text. The same exponential function was applied to the time course of the current measured in 100 μM bicuculline-m and the IC_{50} allowing only the amplitude to change by fixing the exponential time constants to that determined for control values (continuous lines through closed squares in upper panel and closed circles in lower panel, respectively)

trol values obtained immediately before and after each response, and a single binding isotherm was fit to the normalized data. The equation used was $(f_c - f_i) \cdot \text{IC}_{50} / (x + \text{IC}_{50}) + f_i$, where x is the concentration of drug, f_c is the normalized control value in the absence of drug, f_i is the fraction of current not blocked by the drug, and IC_{50} is the concentration at half-maximum response; a nonlinear least-squares procedure was used to determine f_c , f_i , and IC_{50} . All data points are presented as mean \pm SD of n experiments as indicated. Statistical differences were determined using an unpaired t -test; p values < 0.05 were considered significant. Bicuculline free base and methylchloride (bicuculline-m), and picrotoxin were purchased from RBI (Natick, Mass., USA).

Results

Bicuculline blocks SK channels

SK channels were expressed in *Xenopus* oocytes and outside-out patches were examined using symmetrical 120 mM K^+ solutions and a saturating concentration of Ca^{2+} (10 μM) in the patch pipette internal solution; currents were evoked by voltage ramp commands. Application of bicuculline-m in the solution bathing outside-out patches from oocytes expressing apamin-sensitive SK2 channels resulted in a concentration-dependent inhibition of the current measured at -60 mV, with an $\text{IC}_{50} = 1.1 \pm 0.1$ μM ($n=3$); representative current traces

and concentration/response curves are shown in Fig. 1A, B. SK currents in excised patches demonstrate run down as a function of time after patch excision which varied with oocyte batch and was different among the cloned SK channels; in general the extent of run down of SK2 is only modest (closed circles, Fig. 1C) [13]. Initial experiments suggested that bicuculline-m block changes with time after patch excision. Indeed, when current amplitude and block were examined at different time points after patch excision (open circles, Fig. 1C), the data showed that blocking potency decreases slightly in parallel with run down (Fig. 1B, C). For the representative patch shown in Fig. 1, SK2 currents diminished 11% over 21 min and the IC_{50} increased from 1.1 to 1.8 μM . On average the IC_{50} increased from 1.1 ± 0.1 μM to 1.7 ± 0.3 μM over 21 min ($n=3$) and the run down was $9 \pm 5\%$. Experiments performed using physiological ionic conditions (5 mM K^+ in the extracellular solution and 120 mM K^+ in the intracellular solution) yielded similar results (IC_{50} at 0 mV = 1.3 ± 0.2 μM ; $n=3$). These data show that bicuculline-m blocks SK2 channels at concentrations which are routinely used in brain slice experiments to block GABA_A receptor channels (10 μM).

Apamin-insensitive SK1 currents are also blocked by bicuculline-m when applied to outside-out patches im-

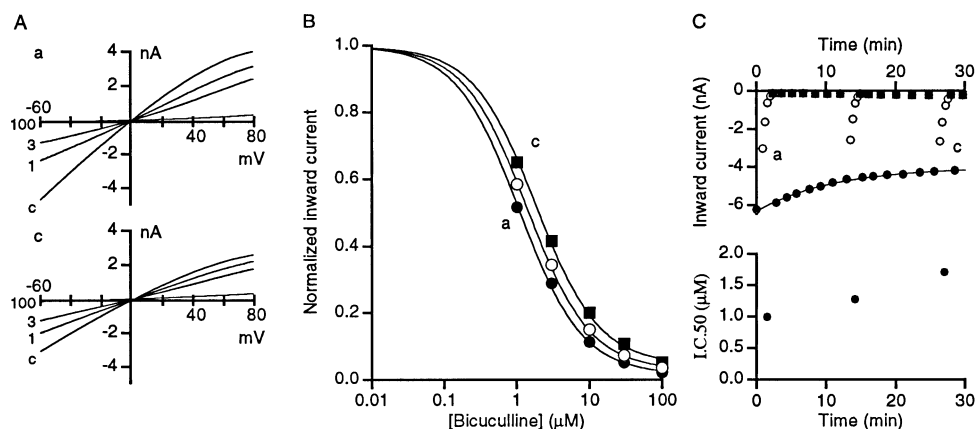
mediately after excision, and concentration/response experiments measured at -60 mV yielded an IC_{50} of 1.4 ± 0.4 μ M, $n=4$; not markedly different than for SK2 ($p=0.4$). SK1 currents undergo a greater degree of run down than SK2 currents ([13]; Fig. 2C). As shown in the example in Fig. 2C, the current measured at -60 mV (closed circles) initially increased immediately following patch excision and was then followed by run down; the time course could be described by a sum of two exponentials (solid line), one for the increasing and one for the decreasing phase. Currents within a concentration response obtained early after patch excision were subject to run down which would bias the IC_{50} . Therefore, current amplitudes were corrected for run down by normalizing to the control current predicted from the time course of run down.

Figure 2B shows concentration/response curves to bicuculline-m measured at different times following patch excision. Initially, SK1 currents were as sensitive to bicuculline-m as SK2 currents, but the IC_{50} increased over time and by the end of the experiment (98 min after patch excision) the IC_{50} was 8.4 μ M (Fig. 2B, C). Associated with the decreased affinity between bicuculline-m and SK1, the fraction of current not blocked by 100 μ M bicuculline-m increased (Fig. 2C, closed squares). Concentrations greater than 100 μ M have not been evaluated but, based on the fits of a single binding isotherm to the concentration response, the fraction of SK1 current not blocked by bicuculline-m (100 μ M) increased from 0.06 to 0.44 . The increase in the IC_{50} for bicuculline-m appeared to parallel the time course of run down. On average the increase in IC_{50} from 1.4 ± 0.4 μ M to 24.4 ± 19.8 μ M was associated with a run down of $66 \pm 22\%$ over 32 – 98 min ($n=4$) while the fraction of current not blocked by bicuculline-m increased from 0.11 ± 0.05 to 0.48 ± 0.21 . The bicuculline-m-resistant current reflects a fraction of SK channels not blocked by bicuculline-m because substitution of external K^+ for Na^+ eliminated the residual inward current in the presence of 100 μ M bicuculline-m and in inside-out patches removal of Ca^{2+} eliminates the current. These data show that SK1 and SK2 are equally sensitive to bicuculline-m but that over time SK1 currents run down and the block by bicuculline-m decreases.

The rate of current run down of SK1 is strikingly similar to the time course of increase of the IC_{50} suggesting that these processes are linked (Fig. 2C). Although the molecular mechanisms responsible for SK channel run down are not known, the decrease in the current with time might result from a shift in the Ca^{2+} sensitivity of the channels and a reduction in open probability. Therefore, the Ca^{2+} sensitivity of the channels was examined immediately and 20 min after excision of inside-out patches; however, no shift in the Ca^{2+} concentration/response curve was observed for SK1 and SK2 (data not shown).

To determine whether bicuculline-m is an open channel blocker, bicuculline block was examined using 0.3 μ M Ca^{2+} in the patch pipette (internal solution), a concentration close to the IC_{50} [16,39] where the open probability of the channels will be reduced compared to the saturating concentrations used in the previous experiments. Under these conditions, bicuculline-m concentration/response measurements show that the IC_{50} is not different to when 10 μ M Ca^{2+} was present in the patch pipette (1.5 ± 0.1 μ M; $n=2$, $p=0.8$).

Fig. 3A–C Mutations E330D, H357N in the outer vestibule of SK1 reduce the time-dependent shift of bicuculline-m-induced block of SK1. **A** Current traces elicited by a 2-s voltage ramp from -60 to 80 mV from an outside out macropatch excised from an oocyte expressing SK1 (E330D,H357N). The traces were obtained in control solution (*c*) and in the presence of 1, 3, and 100 μ M bicuculline-m (labeled accordingly) within the first 2 min (*a*) and 28 min (*c*) following patch excision. **B** Bicuculline-m concentration/response curves measured at three times following patch excision (response curves labeled *a* and *c* correspond to concentration/response traces in panel **Aa** and **Ac**, respectively and to time points labeled *a* and *c* in panel **C**). The IC_{50} for the three series were 1.1, 1.4 and 1.8 μ M for *a*, *b* and *c*, respectively and the fraction of current not blocked by bicuculline-m increased from 0.02 to 0.05. **C** Inward current recorded at -60 mV (upper panel) and IC_{50} (lower panel) as a function of time following patch excision. Plotted are current values in control solution (closed circles), 100 μ M bicuculline-m (closed squares) and three concentrations/response curves to 1, 3, 10, and 30 μ M bicuculline-m (open circles). The first and last series are indicated by *a* and *c*



Residues influencing run down and reduced bicuculline sensitivity

Two amino acids residing on opposite sides of the deep pore are responsible for apamin-induced block of SK2 channels, and substitution of these residues into SK1 endows apamin sensitivity [13]. In the course of those previous studies it was noticed that the doubly mutated, apamin-sensitive SK1 channels (E330D, H357N) also showed reduced run down (unpublished observation). Therefore, the bicuculline-m sensitivity of SK1 (E330D, H357N) currents was examined. Bicuculline-m blocks SK1 (E330D, H357N) currents with an IC_{50} not different from that of SK2 or SK1 currents immediately after patch excision (Fig. 3A, B). The average IC_{50} was $0.9 \pm 0.2 \mu\text{M}$ ($n=3$). However, similar to SK2 currents, SK1 (E330D, H357N) currents showed reduced run down ($30 \pm 6\%$) compared to SK1 and stable bicuculline-m sensitivity; the IC_{50} increased to $1.3 \pm 0.5 \mu\text{M}$ over 27 min (Fig. 3B, C).

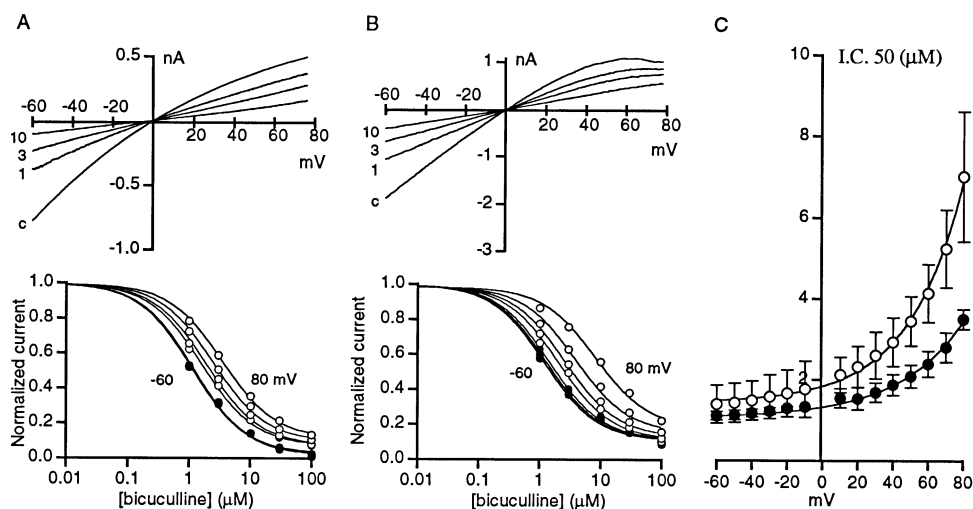
Voltage dependence of bicuculline-m-induced block

Bicuculline-m affected inward currents more than outward currents for both SK1 and SK2 channels (see Figs. 1A, 2A). Therefore, the IC_{50} for bicuculline-m was examined as a function of voltage for SK1 and SK2 (Fig. 4). The concentration/response relationship was determined from a series of voltage ramps for the different concentrations of bicuculline-m by measuring the current at 10-mV increments between -60 and 80 mV (Fig. 4A, B lower panel, respectively; the closed symbols represent inward current and the open symbols represent outward current). The concentration/response at each voltage was fit with a single binding isotherm (see Materials and methods) and the derived IC_{50} was plotted as a function of voltage (Fig. 4C). The results show that for inward currents, at voltages less than 0 mV in symmetrical K^+ , the bicuculline-m IC_{50} changed little as a function of

voltage but significantly increased for outward current as the voltage became positive. The mean data from three patches were fit with a single exponential plus an offset, yielding a voltage dependence of 37.9 mV/e-fold change in the concentration of bicuculline-m for SK2 (Fig. 4C, closed circles), and was 30.7 mV ($n=4$, Fig. 4C, open circles) for SK1. Application of the Woodhull equation [38] suggests that the fraction of the membrane electric field influencing bicuculline-m block (δ) assuming a single charge on bicuculline-m is 0.83 and 0.67 for SK1 and SK2 channels, respectively.

The apparent voltage dependence of bicuculline-m-induced block may result either from an intrinsic voltage dependence or to a “knock-off” effect by K^+ ions passing through the pore [2]. To distinguish between these possibilities, the IC_{50} for bicuculline was determined as a function of voltage when the concentration of K^+ in the internal pipette solution was lowered to 20 mM while the external K^+ concentration was maintained at 120 mM

Fig. 4A–C Voltage dependence of bicuculline-m-induced block of SK2 and SK1. **A** Bicuculline-m concentration/response relationship of SK2. *Upper panel*: current traces elicited by a 2-s voltage ramp from -60 to 80 mV from an outside out macropatch excised from an oocyte expressing SK2. The traces were obtained in control solution (c) and in the presence of 1 , 3 and $10 \mu\text{M}$ bicuculline-m (labeled accordingly) within the first 2 min following patch excision. *Lower panel*: concentration/response curves measured at 20 -mV increments from -60 to 80 mV; concentration/response curves measured for inward and outward currents are displayed with closed and open circles, respectively (the concentration/response curve was not measured at the reversal potential of 0 mV). Nonlinear least-squares fit to a Langmuir isotherm (continuous lines) yielded an increase in IC_{50} from 1.0 at -60 mV to $2.8 \mu\text{M}$ at 80 mV. The fraction of SK2 not blocked by bicuculline-m increased from 0.05 at -60 mV to 0.1 at 80 mV. **B** Bicuculline-m concentration/response relationship of SK1, protocol as described in panel A. The IC_{50} increased from 1.2 at -60 mV to $8.2 \mu\text{M}$ at 80 mV and the fraction of SK1 not blocked by bicuculline-m increased from 0.11 at -60 mV to 0.18 at 80 mV. **C** IC_{50} for SK2 (closed circles, $n=3$) and SK1 (open circles, $n=4$) plotted versus patch potential. The data were fit with a single exponential plus a constant (continuous curve) yielding $1.05 + 0.29 \cdot e^{V/37.9}$ and $1.43 + 0.4 \cdot e^{V/30.7}$ for SK2 and SK1, respectively



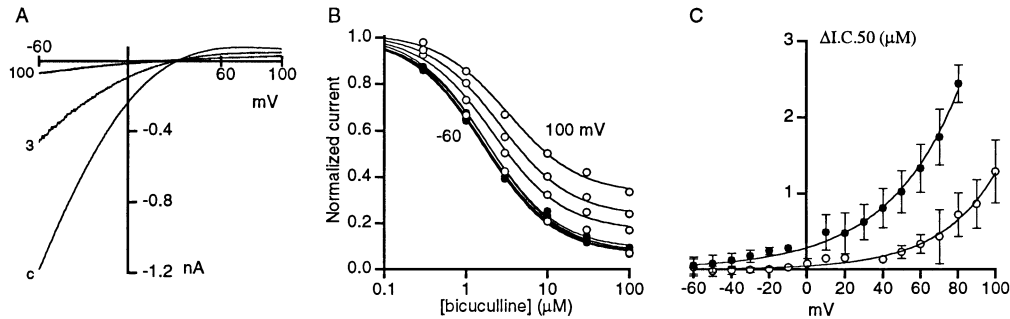


Fig. 5A–C Voltage dependence of bicuculline-m-induced block of SK2 in asymmetrical K^+ . **A** Current traces elicited by a 2-s voltage ramp from -60 to 100 mV from an outside out macropatch containing 20 mM internal K^+ (20 mM K -gluconate, 100 mM Na-gluconate, 5 HEPES, pH 7.2 with $NaOH$) excised from an oocyte expressing SK2. The traces were obtained in control solution (*c*) and in the presence of 3 , and 100 μM bicuculline-m (labeled accordingly) within 2 min following patch excision. **B** Concentration/response curves measured at 20 -mV increments from -60 to 100 mV; concentration/response curves measured for inward and outward currents are displayed with *closed* and *open* circles, re-

spectively. The IC_{50} increased from 1.7 μM at -60 mV to 3.3 μM 100 mV and the fraction of SK2 not blocked by bicuculline-m increased from 0.07 at -60 mV to 0.3 at 100 mV. **C** The change in IC_{50} relative to baseline determined from the exponential fits (ΔIC_{50}) for SK2 in symmetrical 120 mM K^+ (*closed circles*) and asymmetrical K^+ (*open circles*) plotted versus patch potential. The data represent the mean \pm SD for three patches (symmetrical K^+) and two patches (asymmetrical K^+). The absolute values of the IC_{50} were fit with a single exponential plus a constant (*continuous curve*) yielding $1.05+0.29 \cdot e^{V/37.9}$ and $1.72+0.04 \cdot e^{V/30.0}$ for symmetrical and asymmetrical K^+ , respectively

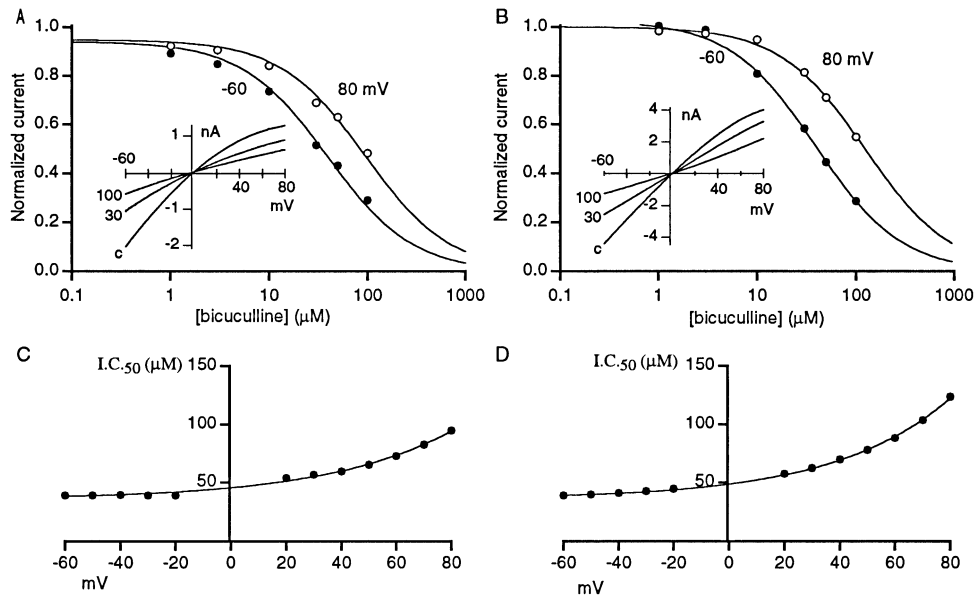


Fig. 6A–D Concentration/response relationship of block of SK2 and SK1 by the free base of bicuculline. **A** Concentration/response curves measured at -60 and 80 mV of SK2. The free base was added from a stock solution of 100 mM in dimethylsulfoxide (*DMSO*). Concentrations greater than 100 μM did not readily dissolve in the recording solution and were not tested. Hence the data were fit with a single Langmuir isotherm with the offset forced to zero. The IC_{50} of block by bicuculline free base increased from 34.4 μM at -60 mV to 76.5 μM at 80 mV. *Inset*: current traces elicited by voltage ramps from -60 to 80 mV in control solution (*c*) and in the presence of 30 , and 100 μM bicuculline (labeled accordingly). **B** Concentration/response curves measured at -60 and 80 mV of SK1. The IC_{50} increased from 38.9 μM at -60 mV to 123.4 μM at 80 mV. *Inset*: current traces elicited by voltage ramps from -60 to 80 mV in control solution (*c*) and in the presence of 30 , and 100 μM bicuculline (labeled accordingly). **C** Voltage dependence of block of SK2 by bicuculline free base. The data were fit with a single exponential function yielding $35.7+10.1 \cdot e^{V/45.5}$. **D** Voltage dependence of block of SK1 by bicuculline free base. The data were fit with a single exponential function yielding $36.3+12.5 \cdot e^{V/41.4}$

(Fig. 5). Figure 5A shows a series of current traces in response to voltage ramps from -60 to 100 mV in different bicuculline-m concentrations with 20 mM K^+ in the patch pipette. Decreasing internal K^+ shifted the reversal potential ≈ 30 mV in the positive direction and decreased the outward current. Concentration/response curves measured at 10 mV increments are shown in Fig. 5B; the increase in unblocked current with increasing voltage probably reflects a greater contribution from leak current at more positive voltages under these conditions in which the outward current is dramatically reduced. The mean IC_{50} for bicuculline-m-induced block of SK2 at -60 mV was 1.7 ± 0.1 μM ($n=2$). To compare the voltage dependence to that in symmetrical K^+ , the IC_{50} was displayed relative to the baseline value (Fig. 5C) and shows that the voltage dependence in low internal K^+ was shifted by ≈ 30 mV compared to that in symmetrical 120 mM

K⁺. This result indicates that at least part of the apparent voltage dependence of bicuculline-m-induced block is due to destabilization of binding by K⁺ ions passing through the pore, a “knock-off” effect, and that bicuculline-m blocks SK channels by a direct occlusion of the pore.

Bicuculline-m block from the inside of the membrane was also examined. Although some sensitivity was observed, it was markedly less than that seen for external bicuculline-m application, with 100 μM blocking 10.08±9.34% (*n*=8) of the inward current at -80 mV and 30.31±11.01% (*n*=8) of the outward current at 80 mV.

The effects of bicuculline free base were also examined. The free base of bicuculline blocked SK1 and SK2 channels but with lower affinity than the methylchloride salt; concentration/response curves measured at -60 mV yielded an average IC₅₀ of 46.3±9.9 μM for SK1 (*n*=5) and 63.3±23.9 μM for SK2 (*n*=3) when examined immediately after patch excision. The block by the free base was voltage dependent with the IC₅₀ increasing between -60 and 80 mV from 34.4 μM to 76.5 μM for SK2 and 38.9 μM to 123.4 μM for SK1 (Fig. 6A, B). When plotted versus patch potential (Fig. 6C, D) the IC₅₀ versus voltage was well described by an exponential function yielding an average voltage dependence of 47.0±8.3 mV (*n*=3) and 41.6±5.9 mV (*n*=5) for SK2 and SK1, respectively. Similar to that observed for the methylchloride salt the IC₅₀ of the free base block of SK1 increased with time following patch excision (data not shown). Thus, at concentrations which effectively block GABA_A receptor channels (10 μM), the free base form of bicuculline will have little effect on SK channels.

Picrotoxin is another widely used compound for inhibition of GABA_A-mediated responses. However, the concentration of picrotoxin generally employed in brain slice experiments (100 μM) did not significantly reduce either SK1 or SK2 currents. At tenfold higher concentrations (1 mM) picrotoxin produced a variable but significant reduction of outward (32±13%, *n*=4; *p*=0.03) and inward (36±15%, *n*=4; *p*=0.02) currents (data not shown).

Discussion

The results presented here demonstrate that bicuculline-m potently blocks cloned SK channels at concentrations routinely employed in brain slice experiments. Therefore, the methyl derivative of bicuculline can no longer be regarded as a selective antagonist of GABA_A receptor channels. As the cloned SK channels probably represent the channels which are responsible for the slow AHP and spike-frequency adaptation in native neurons, the use of bicuculline-m in brain slice experiments may have profound effects on excitability parameters such as firing frequencies and accommodation, compromising interpretations of the role of GABA_A synapses. Similarly, experiments designed to evaluate the AHP in a GABAergic-free background using bicuculline will also be compro-

mised. In contrast, picrotoxin, another commonly employed GABA_A antagonist, has no effect on cloned SK channels at a concentration routinely used for brain slice studies.

Like many channels, cloned SK channels undergo run down following patch excision. The molecular basis for channel run down is not understood but may be due to the loss of associated intracellular second messenger proteins such as protein kinases [6,18], protein phosphatases [26], or inositol phosphates [3, 12,33]. Consistent with this hypothesis, the extent of SK current run down shows considerable variability among different batches of oocytes. There is also an intrinsic distinction between SK1 and SK2 channels as run down is much more pronounced for SK1 channels. Interestingly, for both channels, block by bicuculline-m and bicuculline free base is also altered with time after patch excision, and although there is no clear evidence that run down and altered sensitivity are functionally coupled, in all experiments they correlated well; the extent of current decrease was proportional to the increase of the IC₅₀ for both forms of bicuculline. This suggests that in addition to a decrease in channel activity, run down, presumably initiated by an intracellular process, imposes a slow conformational change on the outer vestibule of the SK channel pore which reduces the affinity for external bicuculline. This process is affected by residues in the outer vestibule of the pore, as substitution of two amino acids from SK2 into SK1 reduced the extent of run down and the shift in the IC₅₀ to that seen for SK2. Immediately after patch excision, SK1 and SK2 channels show similar block by bicuculline-m or free base, suggesting that the molecular determinants for binding are found in both channel types. There are only three amino acid differences in the pore region between SK1 and SK2 [16] and two of these are important for the altered topography of the outer vestibule with time after excision. These results suggest that the pore region is not maintained in a rigid conformation. This is consistent with the observations presented by Guillemare and coworkers who showed that the biophysical properties and sensitivity to neurotoxins of the brain delayed-rectifier K⁺ channels Kv1.2 were affected by the levels of channel expression in *Xenopus* oocytes [10].

Several recent reports have shown that in brain slice experiments bicuculline-m blocks the *I*_{sAHP} [9, 14,31]. However, in some preparations this is clearly not the case. For instance, in whole-cell recordings from hippocampal pyramidal neurons, a prominent apamin-insensitive *I*_{sAHP} remains in the presence of bicuculline-m at concentrations which block the *I*_{sAHP} in other brain regions, and effectively block the cloned channels [26]. Hippocampal pyramidal neurons are one of the few cell types in which only an apamin-insensitive slow AHP has been reported. If SK1 channels underlie the slow AHP in hippocampal pyramidal neurons, then the lack of bicuculline-m sensitivity may indicate that the channels have undergone run down. Further, bicuculline-m application may have obscured an apamin-sensitive slow AHP, simi-

lar to other cell types which demonstrate both components [7, 19, 28,30].

Acknowledgements We thank Dr. Neil Marrion, Dr. Bernd Fakler, and Dr. Paola Pedarzani for fruitful discussions. This work was supported by NIH grants to JPA and JM, and a grant from ICAGEN, Inc.

References

- Adelman JP, Shen KZ, Kavanaugh MP, Warren RA, Wu YN, Lagrutta A, Bond CT, North RA (1992) Calcium-activated potassium channels expressed from cloned complementary DNAs. *Neuron* 9:209–216
- Armstrong CM (1971) Interaction of tetraethylammonium ion derivatives with the potassium channels of giant axons. *J Gen Physiol* 58:413–437
- Baukowitz T, Schulte U, Oliver D, Herlitze S, Krauter T, Tucker SJ, Ruppersberg JP, Fakler B (1998) PIP₂ and PIP as determinants for ATP inhibition of KATP channels. *Science* 282:1141–1144
- Blatz AL, Magleby KL (1986) Single apamin-blocked Ca-activated K⁺ channels of small conductance in cultured rat skeletal muscle. *Nature* 323:718–720
- Chu Z, Hablitz JJ (1998) Activation of group I mGluRs increases spontaneous IPSC frequency in rat frontal cortex. *J Neurophysiol* 80:621–627
- Chung SK, Reinhart PH, Martin BL, Brautigam D, Levitan IB (1991) Protein kinase activity closely associated with a reconstituted calcium-activated potassium channel. *Science* 253:560–562
- Constanti A, Sim JA (1987) Calcium-dependent potassium conductance in guinea-pig olfactory cortex neurones in vitro. *J Physiol (Lond)* 387:173–194
- Dawson RMC, Elliot DC, Elliot WH, Jones UM (1969) Data for biochemical research. Oxford University Press, New York
- Debarbieux F, Brunton J, Charpak S (1998) Effect of bicuculline on thalamic activity: a direct blockade of IAHP in reticularis neurons. *J Neurophysiol* 79:2911–2918
- Guillemare E, Honore E, Pradier L, Lesage F, Schweitz H, Attali B, Barhanin J, Lazdunski M (1992) Effects of the level of mRNA expression on biophysical properties, sensitivity to neurotoxins, and regulation of the brain delayed-rectifier K⁺ channels Kv1.2. *Biochemistry* 31:12463–12468
- Hille B (1992) Ionic channels of excitable membranes. Sinauer Associates, Sunderland, Mass.
- Huang C, Feng S, Hilgemann DW (1998) Direct activation of inward rectifier potassium channels by PIP₂ and its stabilization by Gβγ. *Nature* 391:803–806
- Ishii TM, Maylie J, Adelman JP (1997) Determinants of apamin and d-tubocurarine block in SK potassium channels. *J Biol Chem* 272:23195–23200
- Johnson SW, Seutin V (1997) Bicuculline methiodide potentiates NMDA-dependent burst firing in rat dopamine neurons by blocking apamin-sensitive Ca²⁺-activated K⁺ currents. *Neurosci Lett* 231:13–16
- Kim U, Sanchez-Vives MV, McCormick DA (1997) Functional dynamics of GABAergic inhibition in the thalamus. *Science* 278:130–133
- Köhler M, Hirschberg B, Bond CT, Kinzie JM, Marrion NV, Maylie J, Adelman JP (1996) Small-conductance, calcium-activated potassium channels from mammalian brain. *Science* 273:1709–1714
- Lancaster B, Adams PR (1986) Calcium-dependent current generating the afterhyperpolarization of hippocampal neurons. *J Neurophysiol* 55:1268–1282
- Levitan IB (1985) Phosphorylation of ion channels. *J Membr Biol* 87:177–90
- Lorenzon NM, Foehring RC (1992) Relationship between repetitive firing and afterhyperpolarizations in human neocortical neurons. *J Neurophysiol* 67:350–363
- Madison DV, Nicoll RA (1986) Actions of noradrenaline recorded intracellularly in rat hippocampal CA1 pyramidal neurons in vitro. *J Physiol (Lond)* 372:221–244
- Martell AE, Smith RM (1974) Critical stability constants, volume; Vol. 1, Amino acids. Plenum, New York
- Muramatsu M, Lapiz MDS, Tanaka E, Grenhoff J (1998) Serotonin inhibits synaptic glutamate currents in rat nucleus accumbens neurons via presynaptic 5HT_{1B} receptors. *Eur J Neurosci* 10:2371–2379
- Nicoll RA (1988) The coupling of neurotransmitter receptors to ion channels in the brain. *Science* 241:545–551
- Park YB (1994) Ion selectivity and gating of small conductance Ca²⁺-activated K⁺ channels in cultured rat adrenal chromaffin cells. *J Physiol (Lond)* 481:555–570
- Pedarzani P, Storm J (1996) Interactions between α- and β-adrenergic receptor antagonists modulating the slow Ca²⁺-activated K⁺ current IAHP in hippocampal neurons. *Eur J Neurosci* 8:2098–2110
- Pedarzani P, Krause M, Haug T, Storm JF (1998) Modulation of the Ca²⁺-activated K⁺ current sIAHP by a phosphatase-kinase balance under basal conditions in rat CA1 pyramidal neurons. *J Neurophysiol* 79:3252–3256
- Sah P (1996) Ca²⁺-activated K⁺ currents in neurons: types, physiological roles and modulation. *Trends Neurosci* 4:150–154
- Sah P, McLachlan EM (1991) Ca²⁺-activated K⁺ currents underlying the afterhyperpolarization in guinea pig vagal neurons: a role for Ca²⁺-activated Ca²⁺ release. *Neuron* 7:257–264
- Sah P, McLachlan EM (1992) Potassium currents contributing to action potential repolarization and the afterhyperpolarization in rat vagal motoneurons. *J Neurophysiol* 68:1834–1841
- Schwindt PC, Spain WJ, Crill WE (1992) Calcium-dependent potassium currents in neurons from cat sensorimotor cortex. *J Neurophysiol* 67:216–226
- Seutin V, Scuvee-Moreau J, Dresse A (1997) Evidence for a non-GABAergic action of quaternary salts of bicuculline on dopaminergic neurones. *Neuropharmacology* 36:1653–1657
- Shinohara S, Kawasaki K (1997) Electrophysiological changes in rat hippocampal pyramidal neurons produced by cholecystokinin octapeptide. *Neuroscience* 78:1005–1016
- Shyng S-Y, Nicols CG (1998) Membrane phospholipid control of nucleotide sensitivity of KATP channels. *Science* 282:1138–1141
- Tanabe M, Gähwiler BH, Gerber U (1998) L-type calcium channels mediate the slow Ca²⁺-dependent afterhyperpolarization current in rat CA3 pyramidal cells in vitro. *J Neurophysiol* 80:2268–2273
- Tempie F, Miniaci MC, Anchisi D, Strata P (1998) Postsynaptic current mediated by metabotropic glutamate receptors in cerebellar purkinje cells. *J Neurophysiol* 80:520–528
- Ulrich D, Huganard JR (1997) Nucleus-specific chloride homeostasis in rat thalamus. *J Neurosci* 17:2348–2354
- Wong WT, Sanes JR, Wong ROL (1998) Developmentally regulated spontaneous activity in the embryonic chick retina. *J Neurosci* 18:8839–8852
- Woodhull AM (1973) Ionic blockage of sodium channels in nerve. *J Gen Physiol* 61:687–708
- Xia X-M, Fakler B, Rivard A, Wayman G, Johnson-Pais T, Keen JE, Ishii T, Hirschberg B, Bond CT, Lutsenko S, Maylie J, Adelman JP (1998) Mechanism of calcium gating in small-conductance calcium-activated potassium channels. *Nature* 395:503–507
- Zhang L, McBain CJ (1995) Potassium conductances underlying repolarization and afterhyperpolarization in rat CA1 hippocampal interneurons. *J Physiol (Lond)* 488:661–672